Lund University

Faculty of Science — Physics

Division of Synchrotron Radiation Research

An STM-based study of Bi deposition on InAs(110)

Author:

Tobias Alpskog

Supervisor:

Rainer Timm

Co-supervisor:

Sandra Benter

Thesis submitted for the degree of Bachelor of Science

Project duration: 2 months

January 2020

LUNDS UNIVERSITET

Contents

Abstract

III-V semiconductor compounds containing Bi, such as InBi, have recently attracted much attention due to predictions of band inversion and topological insulators. The predictions showed that films of InBi could be applicable in quantum computers and at room temperature. The common approach of realizing such a structure, by growing InAsBi films, has not been successful, as the Bi content has been far too low for the properties of interest to emerge.

The work presented in this thesis explores an alternative approach to forming the InBi films – with a clean InAs(110) sample as a starting point. Bi is deposited onto the sample via thermal evaporation, keeping the sample at room temperature. If successful, the Bi atoms are believed to undergo an exchange process where they replace the exposed As atoms in the lattice. This would, in turn, enable us to facilitate a higher and more homogeneous Bi incorporation as well as providing an atomically sharp interface between the top layer and the rest of the substrate. The main goal was, therefore, to determine whether the Bi atoms would be incorporated into the host lattice via the Bi-for-As exchange process, or if they would be desorbed and leave the surface. The idea of the exchange process is supported by the previous work on Sb deposition on GaAs and InAs nanowires.

The InAs(110) sample, and the effect of the Bi deposition approach, was studied by scanning tunneling microscopy (STM). By studying the STM images taken, it became evident that the deposited Bi atoms formed monolayer high islands that had a larger rectangular structure than the underlying substrate. Furthermore, the unit cell of the Bi structure was rotated 35.4° clockwise relative to the InAs(110) unit cell. The different structure, as compared to the substrate, indicated that the islands were metallic Bi.

After the Bi deposition, the InAs(110) sample was annealed. However, with only STM to study the sample, it was difficult to tell whether most of the Bi atoms were desorbed from the surface, exposing a much rougher InAs(110) surface, or, if the Bi had been incorporated either as InBi or $InAs_xBi_{1-x}$.

Populärvetenskaplig sammanfattning

Under andra hälften av 1900-talet applicerades kunskapen av halvledare i form av bland annat transistorer, komponenter i radioapparater, och LED-lampor. Sedan dess har halvledare blivit desto mindre och desto kraftfullare. Persondatorn Apple II, som introducerades 1977 av Steve Wozniak och Steve Jobs, innehöll en processor med cirka 3000 transistorer. Idag rymmer de flesta speldatorer grafikkort som innehåller 7.2 miljarder transistorer. Framtidens datorer, kvantdatorer, kommer att rymma en oerhörd beräkningskraft. Idag existerar ett antal konkurrerande koncept angående hur man bygger en kvantdator. En av dem är att använda sig av halvledarmaterial, vars fördel är skalbarhet. För att förverkliga konceptet krävs emellertid en ökad förståelse av halvledarmaterial med egenskaper som är särskilt användbara inom kvantberäkning.

Det överväldigande antalet halvledarkomponenter i relativt små elektronikenheter möjliggörs av halvledarkomponenternas storlek. De befinner sig på nanometer-skalan och kan därför inte längre ses med hjälp av ett ljusmikroskop. På den här skalan dominerar kvantmekanikens lagar, vilket gör forskning om nya halvledarmaterial särskilt utmanande. Speciella tekniker, som till exempel sveptunnelmikroskopi (STM), måste användas för att kunna studera halvledarmaterialen i detalj. Med STM är det möjligt att utskilja enstaka atomer på ytan av ett halvledarmaterial. Tekniken är därför särskilt lämplig metod att använda för att detaljerat studera ytans struktur.

I det här arbetet har jag använt mig av STM för att studera halvledarmaterialet indiumarsenid (InAs) och hur dess yta påverkas av vismut-deposition (Bi-deposition). Vismut (Bi), i fast tillstånd, uppvärmdes tills det övergick till flytande tillstånd och till sist förångades. Ångan riktades mot provet av InAs med målet att erhålla mindre än ett monolager Bi på dess yta. Studien lade fokus på hur Bi-atomerna band sig till InAs-ytan: om de gjorde det via en utväxlingsprocess där Bi-atomerna ersatte As-atomerna för att skapa ett tunt lager InBi, som förutspåtts vara ett lovande halvledarmaterial vars applikationer inkluderar kvantberäkning, eller om de istället band sig svagt som adsorberade atomer.

STM-bilderna visade mindre än ett monolager av Bi-atomer. Bilderna innehöll också

öar, vars struktur skiljde sig från strukturen av den underliggande ytan. Den nya strukturen tros därför vara relaterad till Bi-atomerna. En föreslagen orientering och storlek på det minsta upprepade mönstret av den Bi-relaterade ytstrukturen presenteras i arbetet. Dessutom diskuteras en förändring av den Bi-relaterade ytstrukturen som konsekvens av uppvärmning av provet. Det krävs emellertid komplementerande mätningar för att urskilja det kemiska tillståndet av ytans Bi-atomer.

Acknowledgements

I would like to use this opportunity to thank my family for their continued support throughout my struggles with this degree. Without them, I would not be who I am today and this thesis would never have been written.

I would like to thank my supervisor and co-supervisor, Rainer Timm and Sandra Benter, for the many lessons they have taught me. You have been incredibly helpful. Thank you to the entirety of the STM group for your helpful comments and for doing your best to answer my many questions. I truly have enjoyed working with all of you and I wish you the very best.

I would also like to thank my dear friend Elijah for his enthusiastic and encouraging spirit. How you can walk around with that enormous brain of yours will forever be a mystery.

I would also like to thank Klara for her infinite source of understanding as well as her incredibly kind and giving soul.

Lastly, I would like to thank myself. For keeping what I promised.

List of Abbreviations

DFT Density functional theory

GaAs Gallium arsenide

InAs Indium arsenide

InAsBi Indium arsenic bismide

InBi Indium bismide

LDOS Local density of states

STM Scanning tunneling microscopy

TI Topological insulator

UHV Ultra high vacuum

XPS X-ray photoelectron spectroscopy

1 Introduction

If you have used any electronic devices today, you have indirectly used a vast amount of semiconductors. Semiconductors have helped to revolutionize our every-day lives, from the invention and continuous improvement of transistors to light-emitting diodes and solar cells. Semiconductors have been researched and developed since the invention of the transistor in the middle of the twentieth century [1]; and today the research is pushing the very limits of our understanding in physics, chemistry, quantum mechanics, and material science. Of particular interest are spintronics and quantum computing, as the computational power of quantum computers will allow for a vast uncharted territory to be explored, as well as allowing us to simulate quantum physics [2].

In 2014, Chuang et al. published a paper in which they presented Density Functional Theory (DFT) calculations that predicted a new class of topological insulators (TIs) [3]. The new class of TIs is believed to consist of group-III binary compositions with bismuth (Bi). Their calculations showed interesting features, such as band inversions with gaps large enough to make the TIs suitable for room temperature applications, in multiple pristine binary compound bi-layers including InBi and GaBi. The research group concluded that InBi and GaBi could be applied in quantum computers. Two ways of how to synthesize group-III Bi films were suggested in the paper: by growing III-Bi films through self-assembly on a substrate that bonds strongly with the film, or to grow the film on a substrate that interacts weakly with the film, via dipole interactions.

Since 2014, material scientists have been trying to understand how to manufacture the group-III Bi composite materials. Attempts have been made in growing InAsBi films, but this approach has been limited both in the amount of incorporated Bi and the way Bi is incorporated, as the Bi atoms tend to form clusters over a certain range of Bi concentration [4]. The work presented in this thesis does not follow the same approach. Instead, it focuses on preparing a clean InAs(110) sample on which Bi is deposited via thermal evaporation. The main idea is that Bi will replace As atoms via Bi-for-As exchange, supported by similar studies made on Sb-for-As exchange on GaAs and InAs nanowires [5].

One of the goals of this thesis is to form an understanding of how to transition from

adsorbed Bi to incorporated Bi. The long-term goal of the suggested approach is to form InBi. If this approach is successful, it will facilitate a higher and more homogeneous Bi incorporation as well as providing an atomically sharp interface between the top layer and the rest of the substrate. This will, in turn, enable complex heterostructures that would have the majority of the charge carrier transport on the surface, which could enhance the electrical conductivity.

2 Theory

This section covers the relevant theory regarding III-V semiconductors, surface structure, surface processes, and the basics of STM imaging. The decision was made early in this work not to go into the behavior of topological insulators; this section does, therefore, not introduce any quantum mechanics beyond quantum tunneling. The reason being, the essence of this work lies entirely in material science and STM, focusing only on Bi incorporation and forming flat InBi terraces.

2.1 III-V semiconductors

Semiconductors are mainly characterized by the gap between the conduction band and the valence band, which is usually smaller than approximately 3 eV [6], although there is no clear size in band gap that marks the transition between semiconductors and insulators. III-V semiconductors are very good to study by STM [7], as the group-III and group-V elements can easily be distinguished from each other. Due to their different electronic properties, different elements interact differently with the tip and this makes them distinguishable in the scanned image. This will be discussed in section 2.3.

2.1.1 Surface structure of InAs(110)

Surfaces are described mathematically by their Bravais lattices, as it compactly describes the periodicity and locations of the surface atoms according to equation 1. The principle is that all atoms in a perfect lattice can be reached through multiples of the lattice vectors $\boldsymbol{a_1}$ and $\boldsymbol{a_2}$:

$$\boldsymbol{R} = m\boldsymbol{a_1} + n\boldsymbol{a_2} \tag{1}$$

Miller indices, $(\boldsymbol{x}, \boldsymbol{y}, \boldsymbol{z})$, are used to describe the crystal planes that make up the surfaces. They are defined as the reciprocal values of the points intersecting the axes [8]. In this work, InAs(110) was used for three reasons. Firstly, it has the same concentration of In and As atoms and is, therefore, electrically neutral. Secondly, nanowires with a zincblende structure usually expose the (110) plane [9], and since the long-term goal

includes nanowire applications, the knowledge, or at least parts of it, obtained from studying this surface is presumably directly transferable to experiments involving nanowires. Lastly, the InAs(110) surface has the same amount of As and In atoms. Thus it does not have any built-in charge and is, therefore, a very stable surface. It is also the surface with the lowest energy. Other surfaces will undergo surface reconstruction to lower the surface energy, but this one will not.

The face-centered cubic (fcc) zincblende structure InAs usually forms in bulk can be seen in figure 1(a). The corresponding atomic rows formed by cutting along the (110) plane can be seen in figure 1(b). The distance A-D corresponds to the lattice constant of InAs, which according to the existing literature is 6.06 Å [10]. The distance A-B is then $\sqrt{2}/2 \times 6.06$ Å$\approx$ 4.3 Å. The atomic rows corresponding to this particular crystal plane are expected to be seen on the substrate in STM images with sufficiently good resolution.

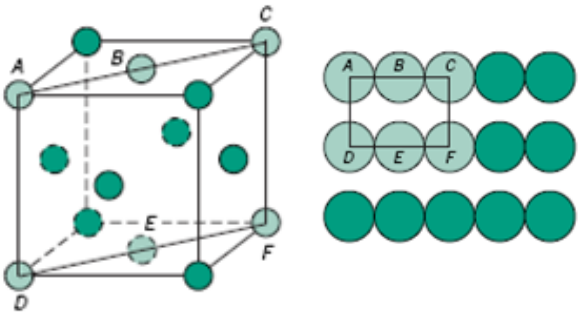

(a) (b)

Figure 1: (a) The zincblende cubic structure that InAs usually forms in bulk, with the corresponding (110) crystal plane that stretches over the atoms A, B, C, D, E and F. (b) The corresponding atomic rows for a (110) surface [11].

Single crystals are used to ensure that experiments are conducted on well-defined surfaces, as a particular crystal plane is exposed given a particular cut through a single crystal. This makes single crystals ideal to use when studying surfaces, as it helps keep the experimental conditions controlled while minimizing the amount of defects that appear on the surface [8].

2.2 Surface processes

When trying to incorporate an element into a composite material, the surface does not stay static. There are several surface processes, such as bonding, diffusion, surface reconstruction, adsorption, and desorption. Each process will affect the topology of the surface in different ways. Below is a summary of the surface processes important to this work. As stated previously, the InAs(110) surface will not undergo reconstruction. Therefore, the process is not of interest here.

Adsorption occurs when atoms form bonds to the surface. The strengths of the bonds may vary and the adsorbates can bind to the surface in various ways. There are two broad classifications of adsorbate bonding; physisorption and chemisorption. The former is weak binding acting over a long-range via dipole interaction with typical binding energies of 10-100 meV per atom, whereas the latter is much stronger, characterized by an exchange of electrons, and with typical binding energies of 1-10 eV per atom. The latter can, therefore, be discussed in terms of the familiar covalent, ionic, and metallic bonding [8].

Diffusion is a process where the adsorbed atoms move across the surface to occupy other hollow sites. For the atom to move to another hollow site, it must cross a so-called bridge site. The bridge site has greater potential energy and the adsorbed atom is, therefore, required to gain a sufficient amount of energy to cross the bridge site. Usually, this occurs via thermal energy [8]. The sample can be annealed at a specific temperature to cause the adsorbed atoms to diffuse and spread across the surface. The temperature at which the annealing is performed can then be varied to achieve different results in terms of the amount of diffusion.

Desorption is the reverse process of adsorption. When the adsorbed atoms are desorbed, they have gained a sufficient amount of energy to leave the surface. Desorption may occur if the sample is annealed at a sufficiently high temperature to cause the bonds between the adsorbate and the surface to break. If the bonds are weak, desorption is more likely to occur. Furthermore, it will occur at lower temperatures than if the bonds were strong. Desorption, as a consequence of annealing, has been observed in the previous work inves-

tigating Bi desorption on InAs(111) [12].

Another process that is of major importance is the Bi-for-As exchange process. It is the process that would allow the Bi atoms to be incorporated into the InAs(110) substrate to form an InBi film. The inspiration and motivation behind why this exchange process can work came from the previous work on Sb-for-As exchange processes on wurtzite/zincblende GaAs nanowires [5].

2.3 STM imaging

STM is a method that measures the quantum tunneling current between a sharp metallic tip and the sample. A schematic of the setup is seen in figure 2. The tip is very close to the surface, without touching it, and it moves over the surface with the help of piezoelectric actuators. A bias is applied over the tip, and the tunneling current, I_T, is measured. The system uses piezoelectric actuators to adjust the distance z between the tip and the surface based on the measured tunneling current.

The scanning can be performed in two modes; constant height and constant current mode. Historically, the former has only been used for atomically flat surfaces. The only advantage of this mode is that because the height is not changed, the operator can obtain a higher scanning frequency. However, the operator still risks crashing the tip into the sample if there is an unexpected height difference on the surface, or if caution is not exercised. The constant current mode is the more common as well as the safer option, as the movement of the tip responds to the change in tunneling current. When the tunneling current increases, the tip is retracted to compensate for the possible height differences on the surface, which prevents the tip from making direct contact with the surface. However, it is also possible that the increase in tunneling current is due to an increase in the local density of states (LDOS), as seen in the increase in height over region B in figure 2. The consequences of an asymmetric tip can also be seen following the dashed line that is the path of the tip. As it travels up over the block in region C, it is rather smooth. However, as the tip moves down from the block, it behaves differently.

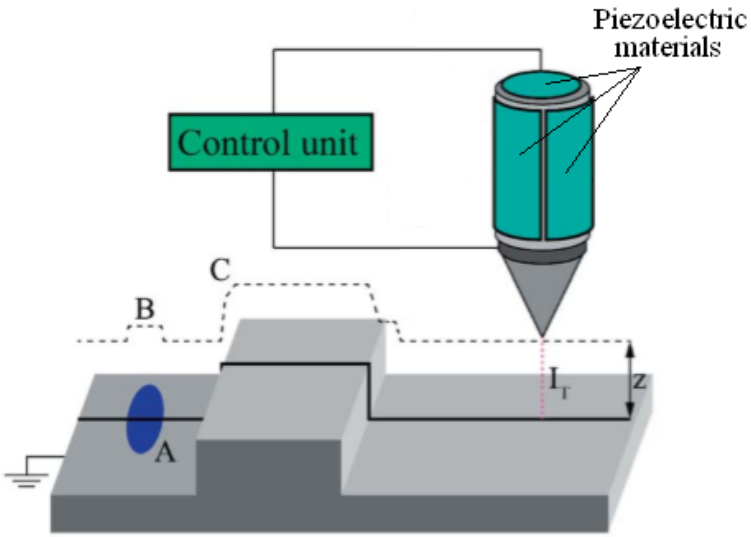

The original schematic was made by Binnig et al. [7] and the figure is based on the version made by J. Knutsson [13].

Figure 2: A schematic representation of the STM setup. Region A represents a change in the LDOS of the sample.

The constant height, on the other hand, is not as dynamic as its counterpart. Here, for example, the height remains constant even if the current increases drastically as the height of the surface spikes. As the height of the tip does not change, the risk of crashing the tip into the sample increases significantly. The constant current mode is, therefore, the mode that was used in this work, as it is far more convenient. In both modes, the piezoelectric materials that adjust the position of the tip in the x-, y-, and z-axis are controlled via a control unit.

The current between the sample and the tip is described by equation 2 below [7]:

$$I \propto e^{-2z\kappa} \tag{2}$$

where z is the separation between the tip and the sample, and κ is the electron decay rate:

$$\kappa = \hbar^{-1}(2m\phi)^{1/2} \tag{3}$$

where $\hbar$ is Planck's constant, m the electron mass and ϕ the effective local work function that depends on the sample bias. Further, Tersoff and Hamann showed that the tunneling current depends on both the LDOS at the tip apex, ρ_t, and the LDOS of the sample, ρ_s,

at energy E and position r according to the following expression [14]:

$$I_T \propto \rho_t \int_{E_F=0}^{eV_t} \rho_{s,loc}(\vec{r_0}, E_F + \epsilon) d\epsilon \tag{4}$$

where E_F is the Fermi level.

As a consequence, the image obtained depends both on the topography of the sample and the material composition. As mentioned previously, the surface in this work is InAs(110). Importantly, there is a noticeable difference in the LDOS between the group-III and group-V elements, where the group-V elements contain more electrons. Furthermore, the group-V elements have more available states for the electrons to occupy. The brightness in the scanned images depends on the polarity of the bias and the imaged atoms. If the applied voltage is negative, the group-III elements will appear dark and the group-V elements will appear bright. The reason why, is that the current flows from the sample to the tip, and the result is what is known as filled-state imaging. The current comes from filled states. As there are more filled states in group-V elements, the atoms corresponding to them appear brighter than the atoms of group-III elements.

3 Experimental method and setup

3.1 The STM instrument

The STM instrument used in this work is an Omicron variable-temperature STM operated at room temperature. It consists of two chambers separated by a valve. First, sample processing is facilitated in the preparation chamber. Afterward, it is transported into the STM chamber where the STM stage and a storage unit are situated. The chamber and the many pumps attached to it are necessary to ensure the ultra-high vacuum (UHV) required to reduce the contamination of the samples. The sample holder and tip are both attached to an anti-vibration stage to reduce vibrational noise. The chamber is, however, not attached to a larger anti-vibration system, and previous work in the lab has, on occasion, suffered from noise due to construction work.

The tip of the STM can be controlled manually, via the Matrix software or a remote control, or automatically, via a feedback-loop integrated with the Matrix software. The manual control is used for coarse movements, to quickly change where the tip is scanning on the surface. The automatic control is limited to changes in the distance between the tip and the sample. The piezoelectric material in the z-direction expands or contracts based on the measured current and the defined loop-gain. The loop-gain is one of the variables that can be specified in the Matrix software (more on this is section 3.5).

Any STM instrument that is not a low-temperature STM with precise temperature regulation will suffer from drift as a consequence of the temperature fluctuations. Unfortunately, the drift is always present without sufficient regulation of the temperature, and it is necessary to consider the amount of drift when choosing the scanning speed. It is also important not to adjust the air-conditioning in the lab, as even a temperature difference of one degree is enough to cause a relatively large amount of drift.

3.2 Sample preparation and cleaning procedure

An InAs(110) wafer was cut to expose the (110) crystal plane. The piece of InAs(110) was held upright, exposing the cross-section, with the help of two supporting pieces on

either side of the sample. The cross-section was then placed on a sample holder to which it was glued in place by heating indium to 200° C.

Once the InAs(110) sample was prepared it was introduced into the UHV system. Since the sample had been exposed to air, the naturally formed oxide had to be removed. The sample was cleaned with atomic hydrogen for 15 minutes. The sample was simultaneously heated up to 395-410 degrees Celsius to increase the temperature and energy possessed by the oxides, thus increasing the probability that the oxides interact with the hydrogen. (The temperature and duration have previously shown to be good values for cleaning semiconducting surfaces without degrading the surfaces [15–17].) Hydrogen gas was fed into a thermal gas cracker, heated up to approximately 1700 degrees C, for cracking hydrogen molecules and providing atomic hydrogen. The complete set of parameters can be seen in Table 1 below. More on the cleaning procedure can be found in the paper by M. Hjort et al. [18].

Table 1: The parameter values used in the cleaning procedure of InAs(110), where the subscript s denotes values of the sample, and the subscript H_2 denotes values of the thermal cracker. The I and V values are the settings of the corresponding power supply.

$I_s = 0.76$ A	$I_{H_2} = 12.4$ A	t = 15 min
$V_s = 13.8$ V	$V_{H_2} = 12.1$ V	p = $5 \cdot 10^{-6}$ mbar
$T_s = 395 - 410$ °C	$T_{H_2} = 1694$ °C	-

3.3 Bi deposition procedure

As mentioned before, Bi was deposited in the preparation chamber. Bi was deposited with the sample at room temperature for 20 minutes by thermally evaporating Bi from a solid source. Solid Bi was placed inside a metal crucible attached to the preparation chamber. A heating filament was wrapped around the metal crucible. The temperature was measured with a type K thermocouple. Further, since Bi transitions to liquid form before transitioning to its gaseous form, the Bi source is anchored at a downward-looking position. The complete set of parameter values for the Bi deposition can be seen in Table 2 below.

Table 2: The parameter values used in the Bi deposition of InAs(110). Here, I_{Bi} and V_{Bi} are the settings of the Bi evaporator power supply.

$I_{Bi} = 6.3$ A	t = 20min
$V_{Bi} = 4.1$ V	p = $1.4 \cdot 10^{-8}$ mbar
$T_{Bi} = 406 \pm 5°$ C	-

3.4 Annealing procedure

The sample was annealed for approximately 5 minutes at a temperature of 285-295° C. We did not want to go to any higher temperatures or longer durations, because then the Bi bonds would break and all the Bi would desorb. The temperature was measured with an infrared thermometer. The temperature fluctuated by a few degrees as the control of the temperature was only indirect. As the time it took to heat the sample to the desired temperature was unknown to the author, the duration likely carries a relatively large uncertainty.

3.5 Data acquisition and data analysis

The data were acquired by using the software Matrix. It is a user-friendly software that allows the user to view the continuous signals, such as the current, coming from the STM instrument while observing the images being scanned in both the forward and backward direction. The quality of the image can be improved further by tweaking the values of several parameters, the most important ones being the scanning speed, scanning area, voltage over the tip and the sample, loop-gain and tunneling current. The raw data, with no operations applied to them, were saved as .mtrix files. After acquiring the raw data, these were analyzed with Gwyddion. Matrix could no longer be used as it only allows for real-time application of a limited number of operations.

4 Results and Discussion

The data acquired and analyzed in this work, in the form of STM images, line profiles, and measurements are presented below. The samples were prepared and studied by STM. Images were taken of the sample after cleaning it, after Bi deposition, and after annealing. This was done systematically in order to obtain similar images that could easily be compared. The samples were then scanned on an increasingly smaller scale. However, difficulties were encountered when attempting to scan on distance 30×30 nm^2 and smaller due to drift. It was especially troublesome scanning over the Bi islands due to the tip interacting unfavourably with the Bi atoms, such as picking them up, causing a change in the LDOS and conductivity of the tip. Eventually, the systematic approach could not be strictly followed. Instead, the guidelines were adapted to obtaining a larger image and a smaller one with high enough resolution to see atomic rows.

4.1 InAs(110) after cleaning with atomic hydrogen

The clean surface can be seen in figure 3 below. It is evident that there are still some bright particles on the surface, which are thought to be oxides. Dark patches can also be seen in the image. As this is a clean InAs(110) sample, the large difference in contrast between the substrate and the dark patches was believed to be due to height differences and not differences in LDOS. Line profiles were extracted from the image to accurately determine the nature of the brighter particles and the patches, as well as to determine the periodicity of the rows. The extracted line profiles can be seen in figures 4-6 below.

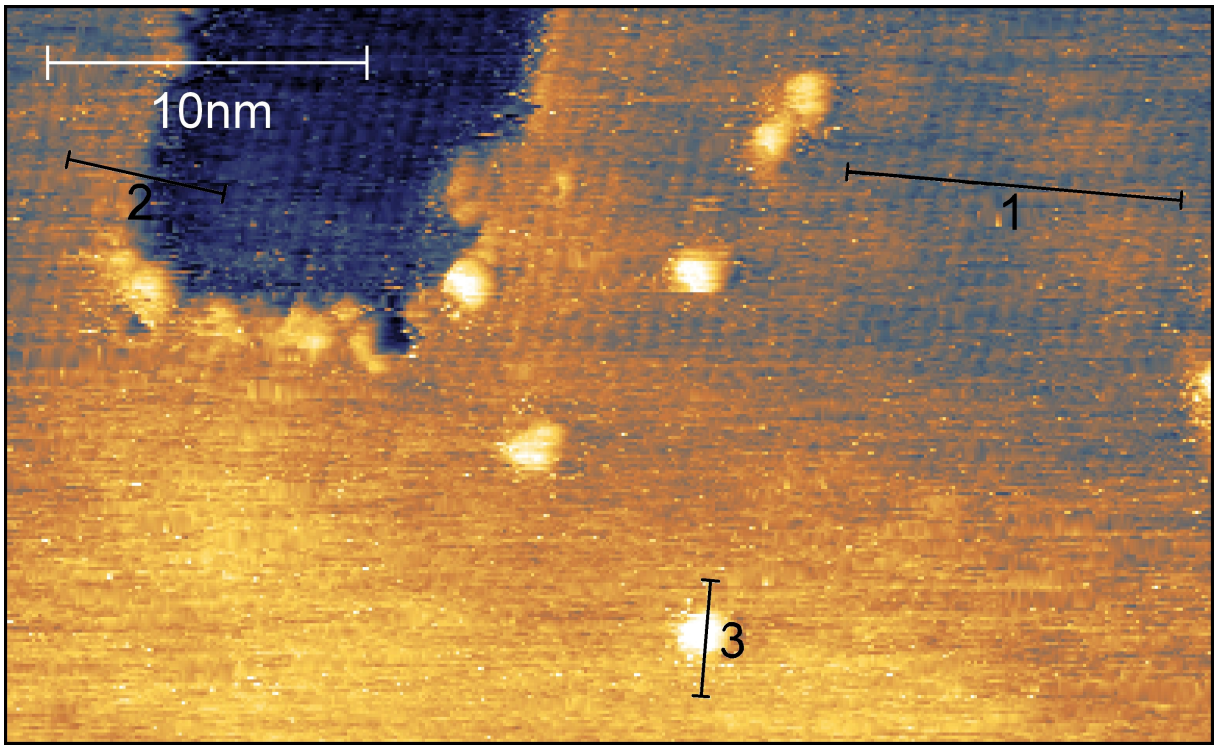

Figure 3: A scanned image of the InAs(110) sample after it had been cleaned with atomic hydrogen for 15 minutes. The positions of line profiles extracted from this image are indicated in black. $V_{gap} = -3$ V, $50x50$ nm^2, $I_T = 100$ pA, loop-gain: 1%, scanning speed: 49 nm/s.

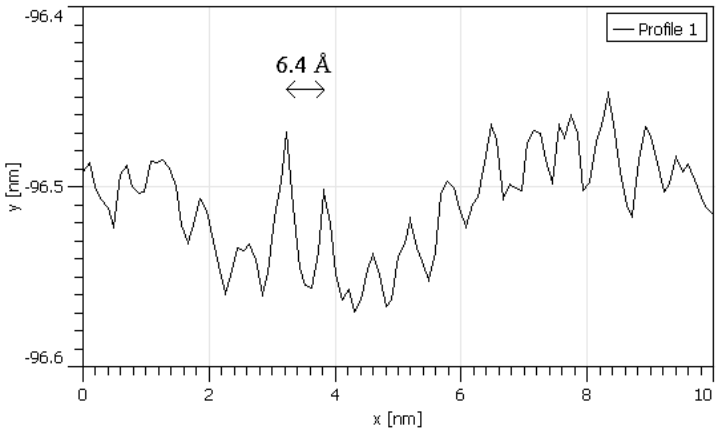

Figure 4: Line profile 1 over the clean InAs(110) rows, extracted from Fig. 3. The average distance between the rows, which was taken over 14 peaks, is indicated in the figure.

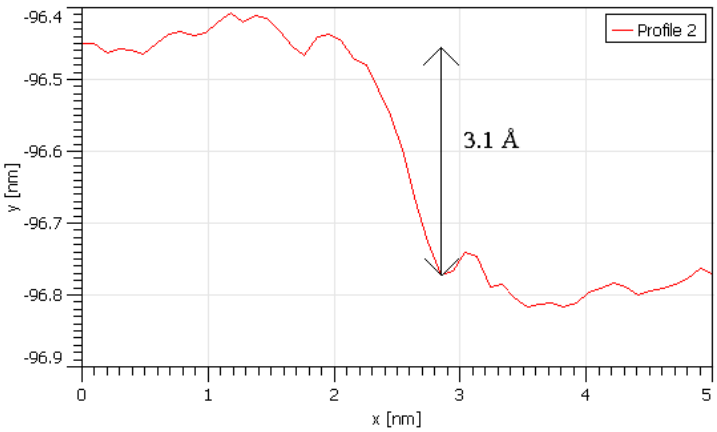

Figure 5: Line profile 2 of the InAs(110) step height, extracted from Fig. 3. The height is indicated in the figure.

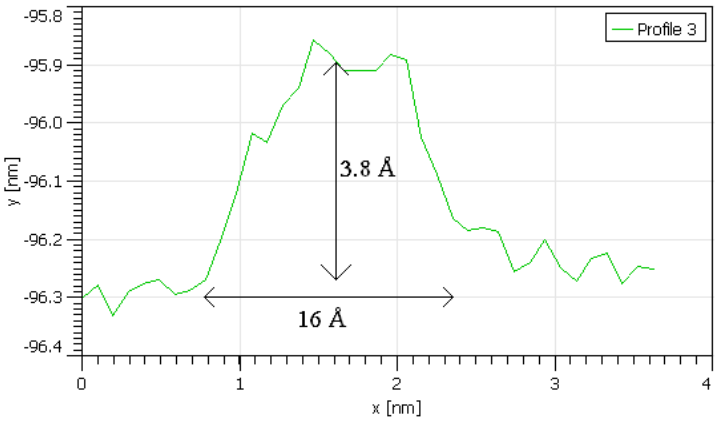

Figure 6: Line profile 3 over the bright particle found on the cleaned InAs(110) sample, extracted from Fig. 3. The height and width is indicated in the figure.

The average distance between the atomic rows of the clean sample is indicated in figure 4. The average was taken over 14 peaks. The experimental result is slightly larger than 6.06 Å, which is the value mentioned in the literature [10]. This could be due to a combination of drift being present in the image and having a slight angle between the line profile and the lattice constant. However, the discrepancy between experimental and literature value is less than 6%.

Figure 5 shows the step height of the InAs(110) sample. The measured height was 3.1 Å, which matches with a monolayer high step.
As can be seen in figure 6, the heights of the bright particles were approximately 3.8 Å. The height is roughly the size of an atom, although the width, 16.0 Å is much larger than

a single atom, more than 4 times as large. What is seen is, therefore, most likely a cluster of oxides that were not removed by the cleaning procedure.

4.2 InAs(110) after Bi deposition

The data presented below are of the InAs(110) surface after 20 minutes of Bi deposition. As can be seen in figure 7, the Bi atoms tend to form large islands on the surface. Line profiles were extracted from the images in order to determine if the islands were monolayer high islands, or if the Bi was incorporated into the surface. Regions, from which line profiles were extracted, are indicated with the red rectangles.

A close-up of region 1 and the corresponding line profiles can be seen in figure 8. The red line profile show that the height of the islands is approximately 2.5 Å, which indicates that the islands are monolayer high islands. If they had not been monolayer high islands, and the Bi had successfully been incorporated into the substrate, the island heights would be expected to be much smaller, with the only difference in height being contributed to the difference in atomic size between Bi and As atoms. The line profiles also indicate that the brighter regions on the islands form a second layer of Bi atoms.

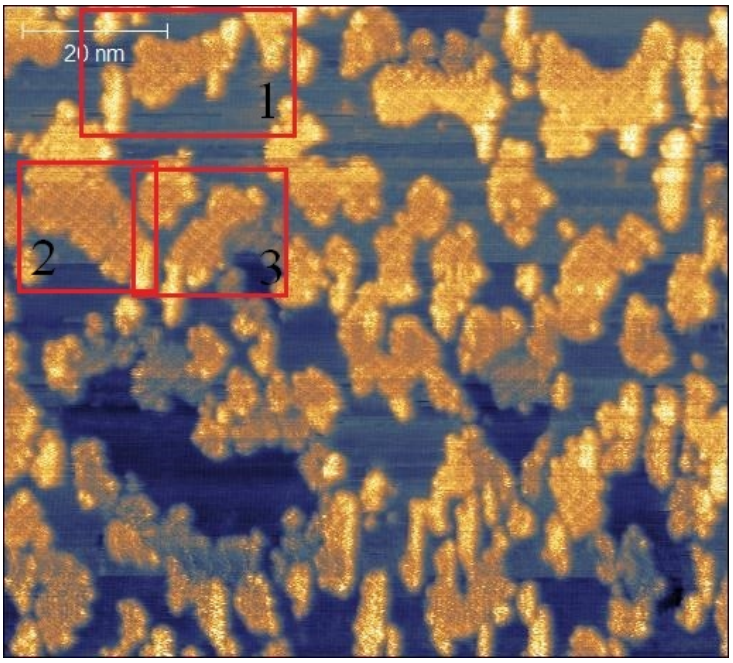

Figure 7: A scanned image of InAs(110) after 20 minutes of Bi deposition. The red rectangles indicate the regions from which line profiles were extracted. $V_{gap} = -3$ V, 100×100 nm^2, $I_T = 30$ pA, loop-gain = 1%, scanning speed: 122 nm/s. Line profiles were applied in the regions marked in red and they can be seen below.

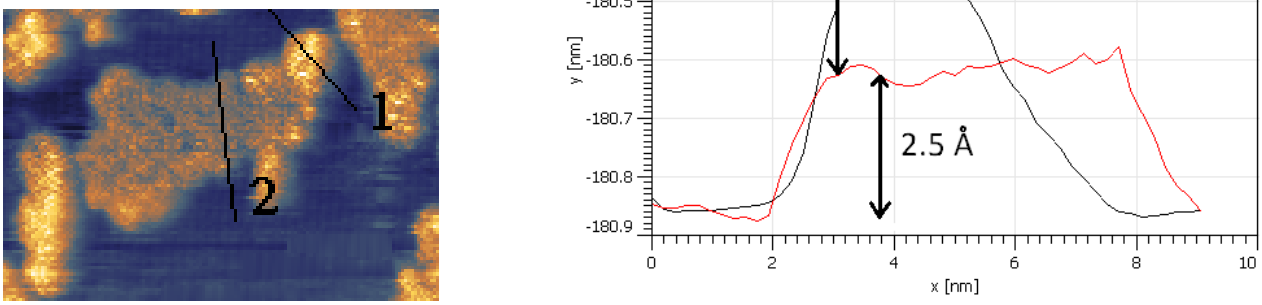

(a) (b)

Figure 8: (a) Shows the positions of the extracted line profiles used to measure the heights of the island. (b) Shows the extracted line profiles and their heights indicated in the figure.

A very interesting feature of the islands is the rectangular pattern that appears on them. The pattern indicates a different surface structure compared to InAs(110). Line profiles were extracted in both directions to obtain the periodicities of the pattern. The line

profiles can be seen in figure 9 and 10, corresponding to region 2 and 3 in figure 7, respectively. The line profiles were taken as an average over the width seen in the image to reduce noise. The average distances between the major peaks can be seen in the figures, and they are 13 Å and 15.7 Å, respectively. These distances are significantly larger than the substrate lattice constant. Therefore, the possibility of the increase in the distance is due to the larger atomic size of Bi can be ruled out, and the islands instead appear to have a structure that is very different from the substrate.

The angles of the Bi structure were measured relative to the rows of the substrate to gain more information about the relative orientation of the Bi unit cell. The angle between the line profile in figure 9 and the rows of the substrate is 32.8°. The angle between the two different lines over the Bi island was measured to be 92.1°. However, the real angle is almost certainly 90°.

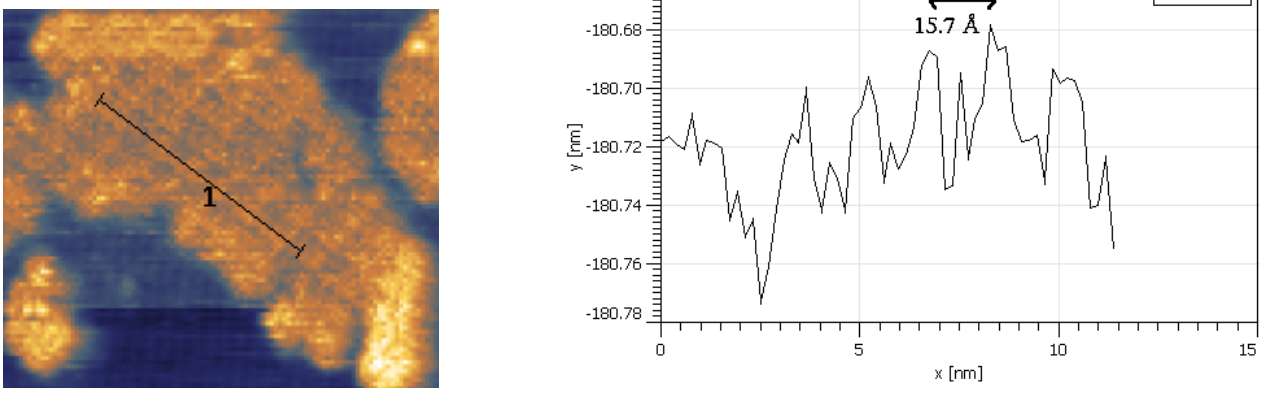

(a) (b)

Figure 9: (a) The position of the line profile used to measure the periodicity of the island along the other direction. The width at both ends indicates the width over which the line profile was averaged. (b) The extracted line profile including the average distance between the larger peaks indicated in the figure. The average distance was taken over 5 peaks.

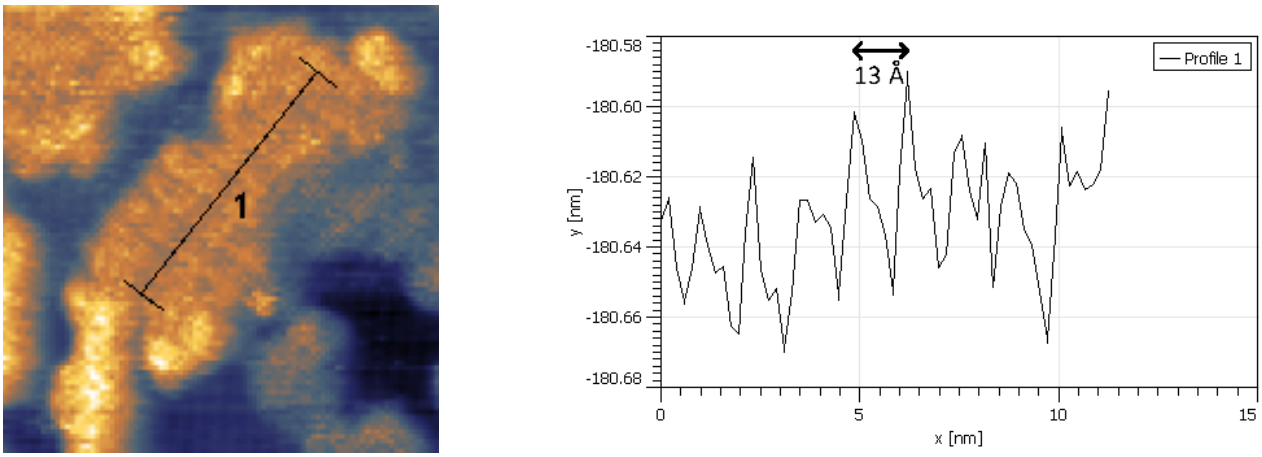

(a) (b)

Figure 10: (a) The position of the line profile used to measure the periodicity. The width at both ends indicates the width over which the line profile was averaged. (b) The extracted line profile including the average distance indicated in the figure. The average distance was taken over 7 peaks.

Given the experimental values of both the distances and the angles, it is possible to speculate about the structure of the Bi unit cell seen on the Bi islands. With the experimental values of the lattice constant obtained from the clean InAs(110) sample, it was found that the Bi structure seen in figure 10 and 9 above may correspond to the structure seen in figure 11 below. This would correspond to distances of 11.0 Å and 15.6 Å. If the literature value of the InAs lattice constant is used, one obtains a distance of 10.6 Å.

The angles of the suggested Bi unit cell would, in turn, correspond to 35.4° and 54.9° compared to the unit vectors of the InAs(110) unit cell, forming a 90.3° angle between the two surface unit vectors. It is, however, difficult to tell the exact Bi structure due to numerous reasons, one of which is the noisy large-scale image. It is a 100×100 nm^2 image. At this scale, each pixel becomes important when studying line profiles such as these. Because of the width, the line profiles were averaged over, multiple smaller peaks are seen in the line profiles. The exact origin of them cannot be determined from the data. Further investigation, such as using a low-temperature STM to reduce the amount of noise and increase the accuracy, is needed to determine the exact orientation and size of the Bi unit cell and the origin of the additional smaller peaks.

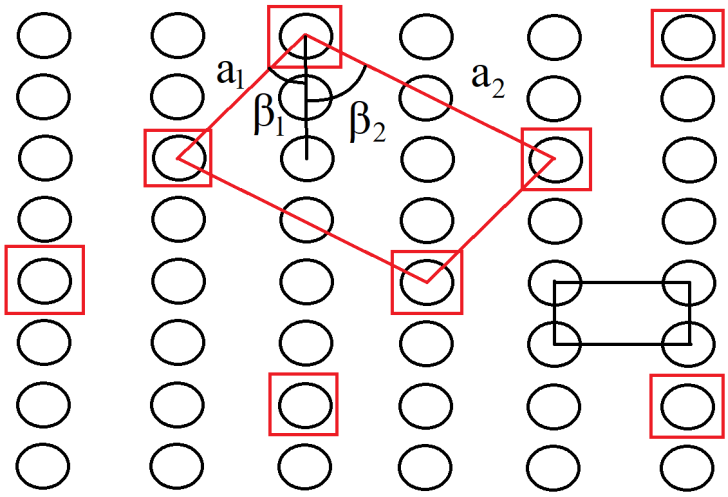

Figure 11: The black circles indicate the underlying As atoms exposed by the (110) plane, and the red squares indicate the Bi atoms positioned on top. The black and red rectangle indicates the As unit cell and Bi unit cell, respectively. $a_1 = 11.0$ Å. $a_2 = 15.6$ Å. $\beta_1 = 35.4°$. $\beta_2 = 54.9°$.

An attempt was made to zoom in on the islands, although it proved to be very difficult as the tip would constantly become unstable over the islands as it interacted unfavorably with the Bi (where the tip picked up atoms and thereby changed the LDOS of the tip). This provided further evidence of the different chemical or electronic properties of the islands as compared to the InAs substrate. However, during this attempt, the substrate was successfully scanned on a smaller scale and lower scanning speed. The image can be seen in figure 12, which depicts what appears to be a square symmetry on the substrate. As was discussed in section 2.1.1, a square symmetry was not expected to be observed on the substrate. Line profiles were applied over the rows in the two directions to determine the experimental value of the distances between the atoms in different directions.

The line profiles in figure 13 showed a shorter distance between the atoms than the previously measured distance between the rows on the clean substrate (6.4 Å). This could be an apparent length compression due to the drift caused by temperature fluctuations in combination with the relatively low scanning speed.

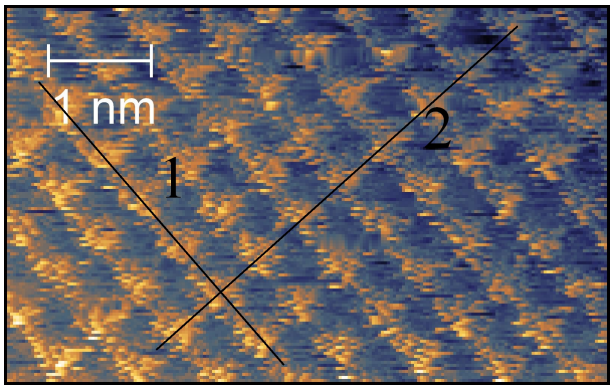

Figure 12: A small-scale image of the InAs(110) substrate after Bi deposition. $V_{gap} = -1.7$ V, 15×15 nm^2, $I_T = 120$ pA, loop-gain: 1%, scanning speed: 37 nm/s.

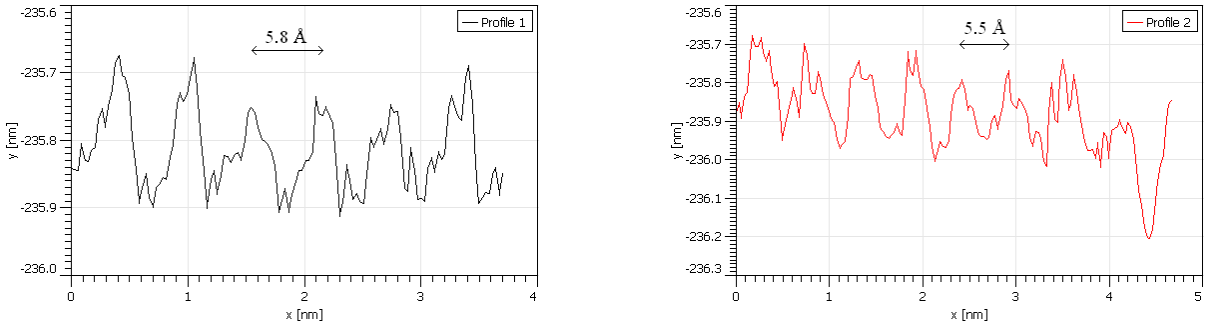

(a) (b)

Figure 13: (a) and (b) are line profiles 1 and 2 from figure 12, respectively. The average distance between the rows is indicated in each figure. The average distances were taken over 6 and 7 peaks, respectively.

4.3 InAs(110) after annealing

Figure 14 shows an image taken of the annealed InAs(110) sample. Atomic rows can be seen on both the substrate and the Bi islands. Line profiles were extracted from the image in order to obtain the periodicity of the rows observed on the substrate and the islands. The line profiles can be seen in figures 15 and 16. An average distance between the rows was measured for each line profile. The average distance between the rows can be seen in each (sub)figure. The range is between 6.6-6.9 Å. This is consistent with the value previously obtained from the clean substrate. This indicates either that the majority of Bi atoms has desorbed from the surface, leaving behind a much rougher surface than expected. Or, the Bi has been incorporated via the Bi-for-As exchange to form an InBi or

an $InAs_xBi_{1-x}$ layer and aligned with the underlying InAs(110) rows. The concentration of the elements in the latter case cannot be found only by using STM.

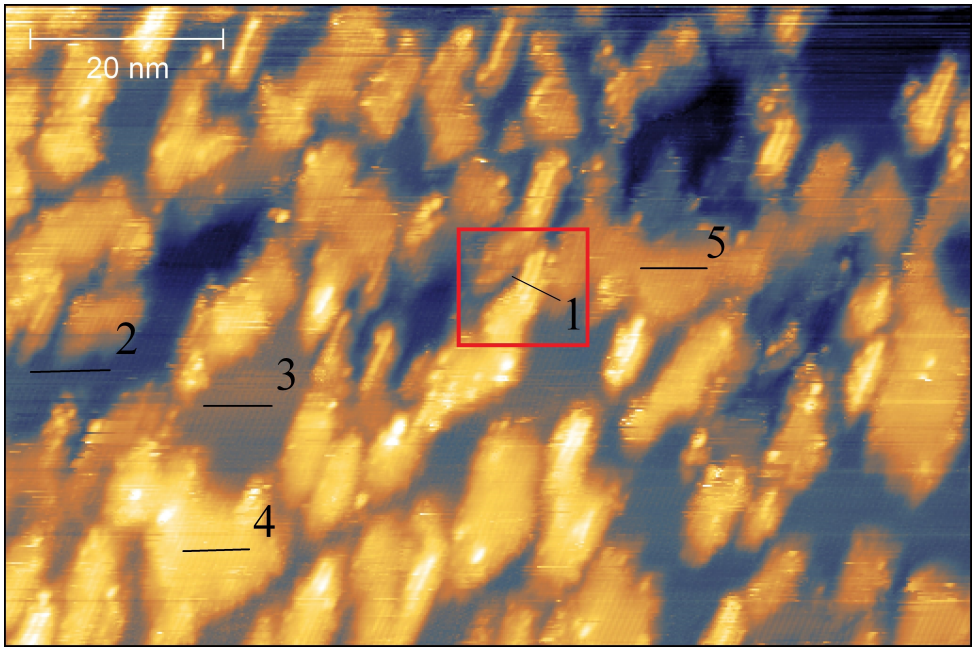

Figure 14: A scanned image of InAs(110) (with Bi deposited on the surface) after annealing. Several line profiles are indicated in the image. Line profiles 2-5 are shown in Fig. 15 and 16. $V_{gap} = -2.7$ V, 100×100 nm^2, $I_T = 130$ pA, loop-gain: 1%, scanning speed: 140 nm/s.

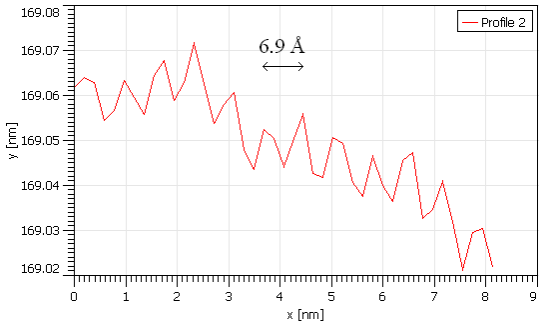

(a)

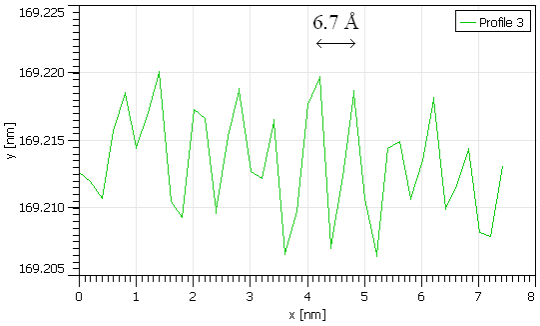

(b)

Figure 15: (a) and (b) are line profile 2 and 3 from Fig. 14. The average distances between the rows are indicated in the images. They were taken over 12 and 10 peaks, respectively.

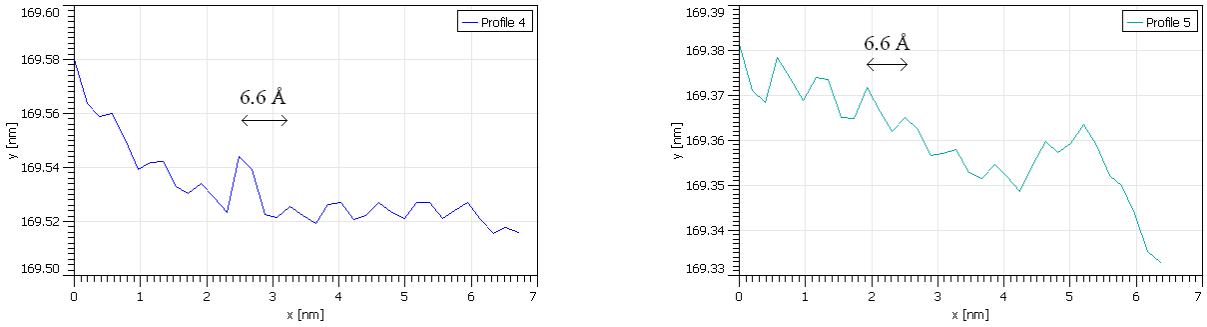

(a) (b)

Figure 16: (a) and (b) are the line profiles 4 and 5 from Fig. 14. The average distances between the rows are indicated in the images. Both of the average distances were taken over 8 peaks.

Slightly thicker and brighter rows can be seen on some of the islands in figure 14. These features indicate that large atoms are sitting on top of the islands. In the extracted line profile seen in figure 17, the total distance between the three brighter rows was measured to be 17.0 Å. According to the line profile, the bright rows are 1.8-2.6 Å above the underlying island. This is roughly the height of the Bi islands seen after Bi deposition, 2.5 Å, indicating that these rare rows are Bi related.

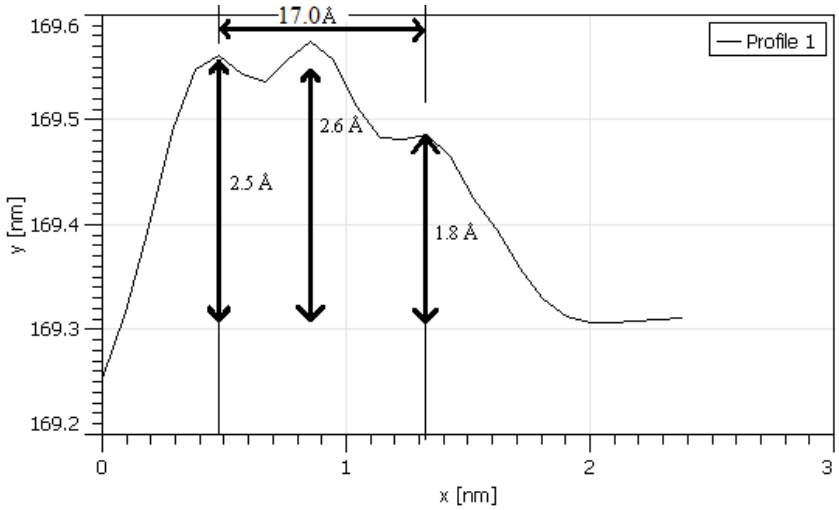

Figure 17: The line profile extracted from the red region in figure 14.

5 Conclusions and Outlook

Atomic rows were observed on the cleaned InAs(110) surface, as well as a few steps and bright particles. The distance between the atomic rows were measured to be 6.4 Å and the step height was 3.1 Å. The bright particles had an apparent height of 3.8 Å and width of 16 Å. The bright particles were, therefore, most likely a cluster of oxidation residue that had not been removed in the cleaning process. The exact nature of the bright particles could be further explored by other techniques, such as x-ray photoelectron spectroscopy (XPS).

Islands could be observed on the surface after Bi deposition. The height-analysis of the islands showed that there were regions on the islands that were 3.2 Å higher than the islands. It is possible that these regions contained clusters of Bi atoms. Furthermore, the islands had a well-ordered Bi-related structure that could very clearly be seen in a scanned image of the size of 100×100 nm^2. A possible overstructure was presented that had reasonable values for both the lattice constants and the angles they formed relative to the orientation of the underlying InAs(110) unit cell. However, this STM does not present enough data to conclusively determine if the suggested overstructure is what was seen. Further data has to be gathered by low-temperature STM, and complementary methods, such as XPS, to decisively conclude the size and orientation of the Bi-related structure and how Bi binds to InAs(110).

After annealing, the surface had changed significantly. The well-ordered Bi-related structure could no longer be observed. It is difficult to tell if the Bi atoms were incorporated to form an InBi film or $InAs_xBi_{1-x}$ film, or if the majority of Bi desorbed. The surface structure resembles that previously seen in the clean InAs(110), albeit a much rougher surface. A few larger atomic rows were observed along the thinner parts of the islands and they are most likely Bi atoms. The amount of Bi and the nature of the bonds between Bi and the substrate is suitably investigated by XPS. Answering the questions left open by this thesis is, therefore, straight-forward as what cannot be determined by the temperature-variable STM can easily be investigated by low-temperature STM and other methods.

References

[1] J. Bardeen and W. H. Brattain. "The transistor, a semi-conductor triode". In: *Physical Review* 74.2 (1948), p. 230.

[2] Y. Wang et al. "Quantum computation and quantum information". In: *Statistical Science* 27.3 (2012), pp. 373–394.

[3] F.-C. Chuang et al. "Prediction of large-gap two-dimensional topological insulators consisting of bilayers of group III elements with Bi". In: *Nano letters* 14.5 (2014), pp. 2505–2508.

[4] L. Wang et al. "Novel dilute bismide, epitaxy, physical properties and device application". In: *Crystals* 7.3 (2017), p. 63.

[5] M. Hjort et al. "Crystal Structure Induced Preferential Surface Alloying of Sb on Wurtzite/Zinc Blende GaAs Nanowires". In: *Nano Letters* 17.6 (2017), pp. 3634–3640.

[6] P. Hofmann. *Solid state physics: an introduction*. John Wiley & Sons, 2015.

[7] G. Binnig et al. "Surface studies by scanning tunneling microscopy". In: *Physical Review Letters* 49.1 (1982), p. 57.

[8] G. Attard and C. Barnes. *Surfaces*. Oxford University Press, 1998.

[9] M. Hjort et al. "Crystal Structure Induced Preferential Surface Alloying of Sb on Wurtzite/Zinc Blende GaAs Nanowires". In: *Nano Letters* 17.6 (2017), pp. 3634–3640.

[10] M. T. Litz et al. "Epitaxy of Zn1- xMgxSeyTe1- y on (100) InAs". In: *Journal of crystal growth* 159.1-4 (1996), pp. 54–57.

[11] W. D. Callister. *Fundamentals of materials science and engineering*. Vol. 471660817.

[12] J.-C. Liu. *The STM Study of Bi Adsorption on the InAs(111)B Surface*. Master Thesis. 2019.

[13] J. Knutsson. *Atomic Scale Characterization of III-V Nanowire Surfaces*. Doctoral Dissertation. Lund University, 2017.

[14] J. Tersoff and D. R. Hamann. "Theory of the scanning tunneling microscope". In: *Physical Review B* 31.2 (1985), p. 805.

[15] G. Bell et al. “Atomic hydrogen cleaning of polar III–V semiconductor surfaces”. In: *Surface Science* 401.2 (1998), pp. 125–137.

[16] T. Kikawa, I. Ochiai, and S. Takatani. “Atomic hydrogen cleaning of GaAs and InP surfaces studied by photoemission spectroscopy”. In: *Surface Science* 316.3 (1994), pp. 238–246.

[17] T. Veal and C. McConville. “Controlled oxide removal for the preparation of damage-free InAs (110) surfaces”. In: *Applied Physics Letters* 77.11 (2000), pp. 1665–1667.

[18] M. Hjort et al. “Surface morphology of Au-free grown nanowires after native oxide removal”. In: *Nanoscale* 7.22 (2015), pp. 9998–10004.